

**WEAKLY NONLINEAR DYNAMIC REGIME: EXTRAORDINARY STIFFNESS
TUNABILITY THROUGH THERMAL EXPANSION OF NONLINEAR DEFECT MODES**

6.1 Introduction

Incremental stiffness characterizes the variation of a material's force response to a small deformation change. Typically materials have an incremental stiffness that is fixed and positive, but recent technologies, such as super-lenses¹⁰⁶, low frequency band-gap materials¹⁷ and acoustic cloaks^{107,108}, are based on materials with zero, negative, or extremely high incremental stiffness. So far, demonstrations of this behavior have been limited either to a narrow range of frequencies¹⁷, temperatures¹⁰⁹, stiffness¹¹⁰ or to specific deformations^{21,111}. Here we demonstrate a mechanism to tune the static incremental stiffness that overcomes those limitations. This tunability is achieved by driving a nonlinear defect mode in a lattice. As in thermal expansion, the defect's vibration amplitude affects the force at the boundary, hence the lattice's stiffness. By using the high sensitivities of nonlinear systems near bifurcation points, we tune the magnitude of the incremental stiffness over a wide range: from positive, to zero, to arbitrarily negative values. The particular deformation where the incremental stiffness is modified can be arbitrarily selected, varying the defect's driving frequency. We demonstrate this experimentally in a compressed array of spheres and propose a general theoretical model. This approach opens a new paradigm to the creation of fully programmable materials.

Research on materials with mechanical properties not found in natural systems is a very active field. This research effort has resulted in different solutions: metamaterials¹⁸, materials undergoing phase transitions^{109,112,113} or buckling instabilities²¹, and materials with

electromagnetic coupling between constituents^{110,114}. Metamaterials are periodic systems with local resonances that can present negative or zero effective mass and stiffness^{17-19,48}; however, their practical application is limited to a narrow band around the local resonance frequency¹⁸. Materials that operate around phase transitions^{112,115} or buckling instabilities²¹ can achieve extreme negative values of the incremental stiffness, but their operation is limited to the deformation or temperature where the instability occurs¹⁰⁹. Negative stiffness inclusions in a matrix, used to achieve positive extreme stiffness, suffer from stability problems¹¹⁶. Finally, many of the proposed solutions are limited in the range of attainable stiffness¹¹⁰.

In order to address those limitations, we demonstrate tuning the incremental stiffness of a lattice using a method based on the thermal expansion of defect modes. Thermal expansion is an ubiquitous property of anharmonic lattices⁹⁵, in which the lattice can be made to expand or contract by increasing or decreasing its vibrational energy. In our method, we drive a defect mode in a lattice with a harmonic signal. As a consequence of anharmonicity in the lattice, an external deformation moves the defect mode in and out of resonance, affecting its vibrational amplitude. These changes in vibrational amplitude affect the thermal expansion of the defect, and therefore the force at the boundary. This alters the incremental stiffness of the lattice. We use this concept to achieve negative stiffness (Fig. 6.1a).

6.2 Tuning the incremental stiffness in a granular chain

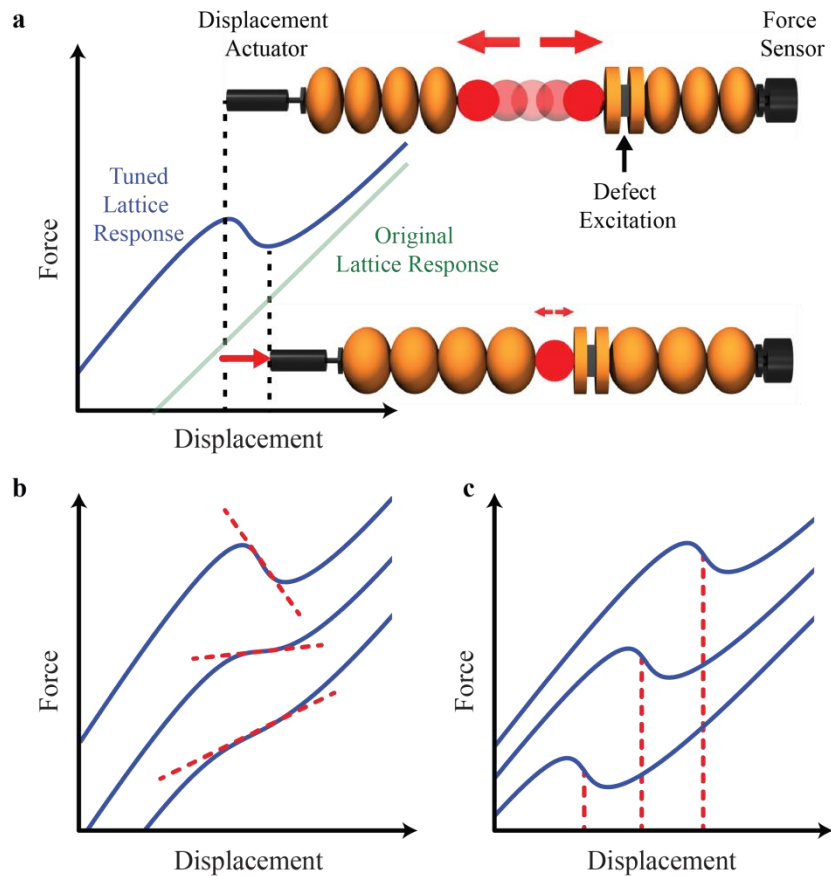


Figure 6.1: Tuning stiffness through thermal expansion. **a.** Schematic diagram of the tunable stiffness mechanism illustrated in a 1-D granular chain. The diagram shows the static force on the lattice due to a prescribed displacement while harmonically driving the defect mode. As the lattice is compressed (blue arrow), the defect vibrational amplitude decreases (red arrows). This results in a negative incremental stiffness due to thermal contraction of the defect mode. **b.** Changes in the driving frequency and amplitude of the excitation control the incremental stiffness, and **c.** the strain point at which the stiffness is being modified. The curves are offset for clarity.

We demonstrate the concept in a one-dimensional lattice of coupled spheres (see Fig. 6.1a). The spheres interact through a nonlinear Hertzian contact²⁷. The central particle is a defect that allows the existence of a localized vibrational mode^{27,117,118}. A piezoelectric actuator is embedded in the vicinity of the defect particle and is used to harmonically excite the defect mode. We monitor the defect mode vibration using a laser vibrometer. We acquire the quasi-

static force-displacement relation of the lattice, by prescribing an external deformation and measuring the force at the opposite boundary. The vibration of the defect mode affects the force-displacement relation. The amplitude and frequency of the defect excitation are the two control variables that determine the mechanical response. Using these variables we can select both the incremental stiffness magnitude (Fig. 6.1b) and the displacement point where the incremental stiffness is being modified (Fig. 6.1c). This allows tuning the force-displacement response of a lattice at a selectable displacement value, a capability that exists so far only in biological organisms¹¹⁹.

In our system the measured force depends on both the applied displacement and on the amplitude of the mode, $F(x, A)$. Therefore, the incremental stiffness, defined as the total derivative of the force with respect to the displacement, is given by the equation:

$$\frac{dF}{dx} = \left(\frac{\partial F}{\partial x}\right)_A + \left(\frac{\partial F}{\partial A}\right)_x \frac{\partial A}{\partial x}. \quad (6.1)$$

The first term on the right side of the equation gives the stiffness of the lattice, neglecting any change in the defect mode's amplitude. The second term describes the effect of the oscillation of the defect mode. The function $(\partial F/\partial A)_x$ is the change in the force due to a change in amplitude of the defect mode and quantifies the intensity of the thermal expansion. From a dynamical point of view, this arises due to an asymmetry of the interaction potential⁹⁵ and in our lattice is always positive (see Appendix, 1.1). Finally, the effect of the strain on the amplitude of the mode is contained in the quantity $\partial A/\partial x$.

The vibration amplitude's dependence on strain is a consequence of the harmonic excitation and of the nonlinearity present in the chain. The harmonic excitation results in a defect mode resonance, which occurs when the defect mode's frequency matches the excitation frequency. The nonlinearity relates the mode's frequency, ω_d , to the lattice strain, δ_0 . In our system the Hertzian contact results in the relationship, $\omega_d \propto \chi_0^{1/4}$. As a result, straining the lattice causes a change in the mode's frequency (Fig. 6.2a). If the mode's frequency approaches the excitation frequency, the mode gets closer to resonance, and therefore the oscillation amplitude increases. Conversely, if the mode frequency moves away from the excitation frequency, the oscillation amplitude decreases (Fig. 6.2b). This strain controlled resonance results in a dependence of amplitude on strain and therefore, in a non-zero $\partial A / \partial \chi$.

Different excitation frequencies cause the resonance to happen at different strain values (Figs 6.2a,b). This is due to aforementioned frequency strain relationship, which associates a particular resonance strain to each excitation frequency. By choosing the excitation frequency we are able to set the displacement region where the system is in resonance and the stiffness is being modified (Fig. 6.2b).

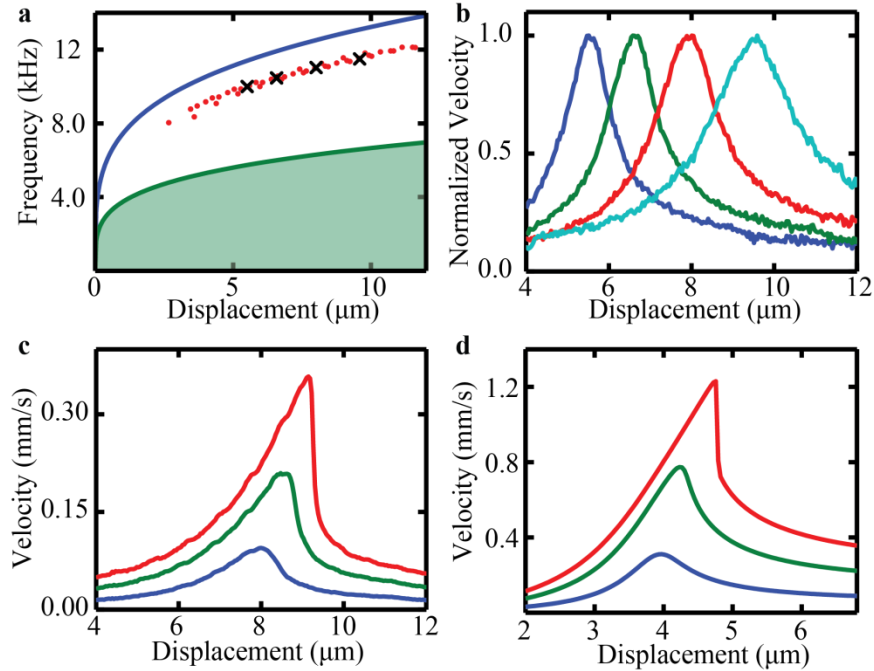


Figure 6.2: Response of the nonlinear defect mode. **a.** Theoretical defect mode (blue) and acoustic band (green) frequencies' dependence on prescribed displacement. Experimental measurements are plotted as red dots with the four curves in panel **b** marked with black crosses. **b.** Normalized experimental velocity of the defect mode as a function of displacement of the lattice. Curves correspond to excitation frequencies of 10(blue), 10.5(green), 11(red), and 11.5 kHz (cyan). **c.** Experimental velocity of the defect mode for drive amplitudes of 4.2 (blue), 9.8 (green), and 15.4 nm (red) all at 10.5 kHz. **d.** Numerical results corresponding to **c**, for defects driven at 20, 50, and 80 nm, respectively. Our simplified model (see Methods) qualitatively reproduces the experimental results, but is unable to make precise quantitative predictions.

The effect of the excitation amplitude on the defect's vibration is shown in Fig. 6.2c,d. As expected, driving the defect with larger harmonic forces results in larger oscillations. Furthermore, as the excitation amplitude gets larger the resonance response becomes increasingly asymmetric. This is a common property of driven nonlinear oscillators close to a bifurcation⁸. As nonlinear system's approach bifurcation points, oscillations become extremely sensitive to the strain¹²⁰; in our system the magnitude of $\partial A/\partial x$ approaches minus infinity. This allows us to achieve arbitrarily large negative values of incremental stiffness.

These extreme negative values have been attained experimentally. The measured force-displacement curves at four different drive amplitudes are shown in Fig. 6.3. The incremental stiffness at our selected strain progressively decreases as the defect excitation is increased (Fig. 6.3a-d). For the largest excitation amplitude, the incremental stiffness reaches negative infinity (Fig. 6.3d). In order to validate that this effect is due to the defect's vibration, we simultaneously measure the defect's mode amplitude, presented below each force-displacement curve in Fig. 6.3a-d. The greatest change in the incremental stiffness happens where the slope, $\partial A/\partial x$, is the most negative. This occurs because larger changes in vibrational amplitude are accompanied by larger changes in thermal expansion. It should be noted that the negative stiffness values are stable because our experiment is done under prescribed displacement boundary conditions.

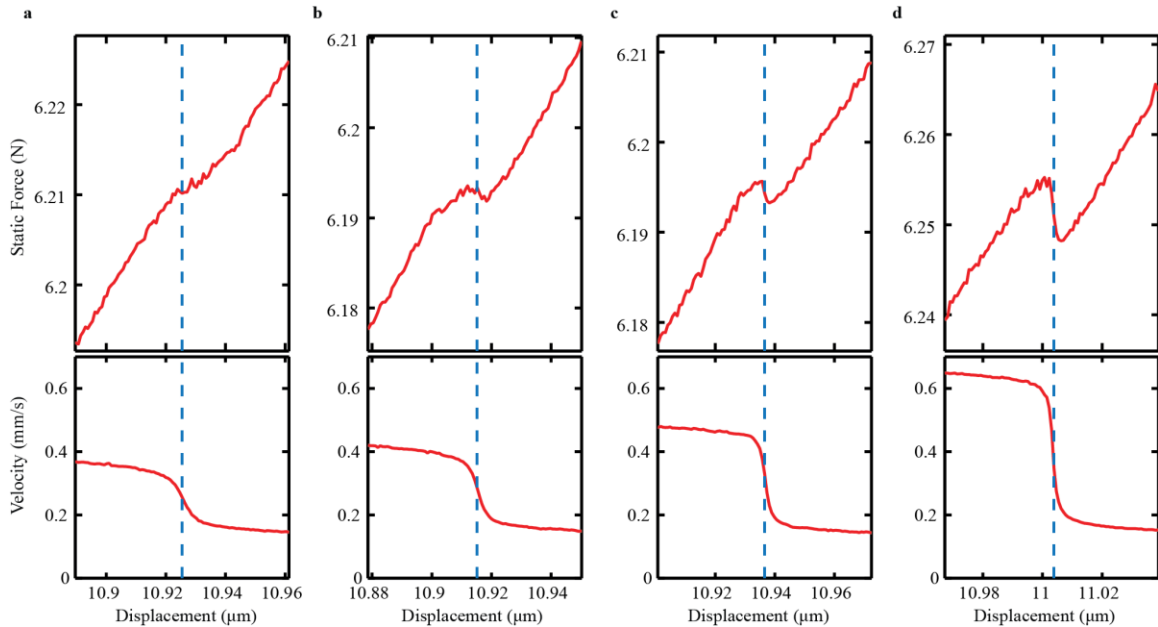


Figure 6.3: Experimental tuning of the incremental stiffness. Force-displacement curves for excitation amplitudes of **a.** 5.9 nm **b.** 6.4 nm **c.** 7.54 nm **d.** 10.9 nm. Shown below are the defect mode velocities (proportional to the mode amplitude, $A(x)$) as a function of the overall displacement, x , of the lattice.

Each pair of drive frequency and amplitude results in a determined incremental stiffness at a particular displacement point. We explore this relationship analytically (see Appendix 1.1) in Fig. 6.4a. The blue lines show contours at the same excitation amplitude and the red lines at the same frequency. To get a particular stiffness at a desired displacement, we select the excitation parameters corresponding to the lines passing through this point. While we only show a finite number of constant lines, all possible values in the shaded region are attainable.

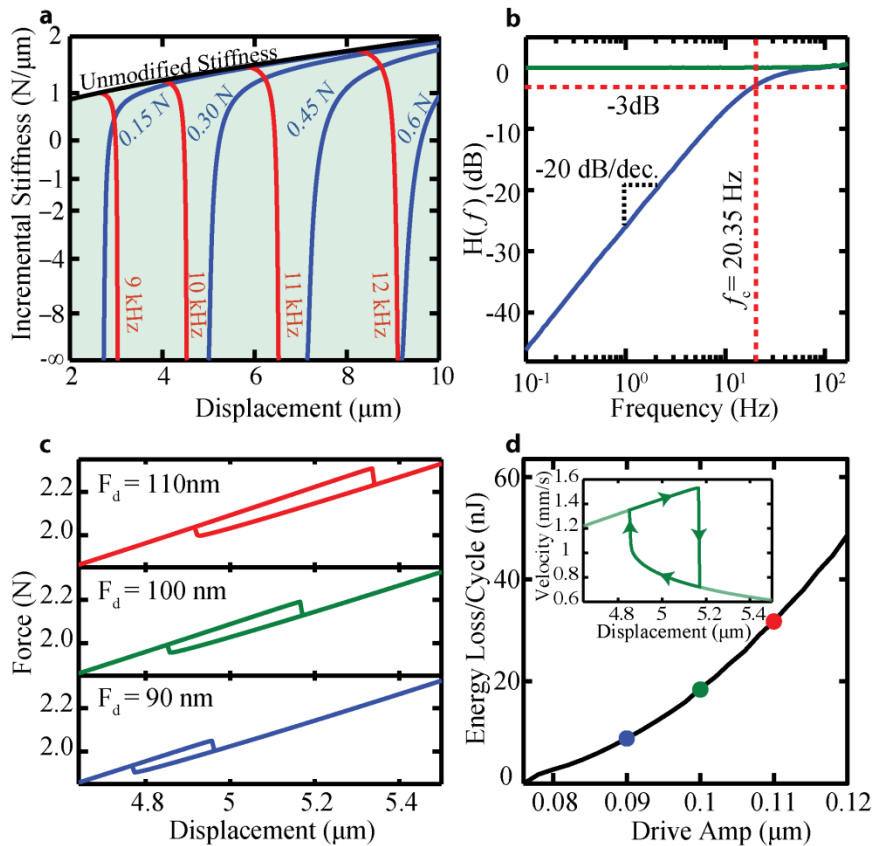


Figure 6.4: Theoretical Investigation. **a.** Map relating the excitation parameters with the modified incremental stiffness and displacement point. **b.** Zero frequency band gap obtained by choosing excitation parameters corresponding to zero stiffness for the lattice. The blue and green line show the force transmitted with the defect drive on and off, respectively. The dotted red line shows the band edge frequency, f_c . When the drive is on, there is a band gap, and when the drive is off the lattice acts as a linear spring. **c.** Force-displacement relationships of the system when it is driven above the bifurcation amplitude. The presence of a tunable hysteresis allows the system to be used as a tunable damper. **d.** As the drive amplitude increases past

the bifurcation, the hysteretic losses per cycle increase. The highlighted points correspond to the results in **c**. The inset in **d** shows the hysteresis in the defect vibration amplitude as the lattice is compressed cyclically.

A remarkable feature of the tuning mechanism presented is that it can achieve zero incremental stiffness. In this region the material will support a load, but it will not transmit any vibration to it, which is of great practical relevance¹²¹. In the zero stiffness region the lattice will have a zero frequency band gap. We simulate this band-gap using our numerical model. In the simulation, we apply a very small amplitude periodic deformation in one end of the chain, and monitor the transmitted force at the other end (Fig 6.4b). We can see that the band gap exists only at low frequencies, and that at high frequency deformations can propagate without attenuation. We quantify the width of the band gap by fitting the transmission to a first order high pass filter, $H(f) = (f/f_c)/\sqrt{1 + (f/f_c)^2}$. This results in a cutoff frequency of $f_c = 20.35 \text{ Hz}$. The upper end of the band-gap is a consequence of the fact that the tuned force versus displacement relationship corresponds to the defect mode oscillating in steady-state. When we change the deformation of the lattice, the steady-state oscillation of the defect is perturbed. The system cannot recover the steady state motion instantaneously. The time it takes for the defect mode to relax back to its steady state limits the upper frequency of the band gap. The speed of the system can be analyzed by using a linear perturbation method (Floquet analysis, see section 6.3).

At the point where the stiffness reaches minus infinity, the dynamics undergoes a bifurcation. At this bifurcation point the system goes from having a single solution to having multiple

stable solutions⁸. This leads to a hysteretic force-displacement response, with the system following different paths when contracting or expanding (Fig. 6.4c). The area of the hysteresis loop corresponds to the loss of energy incurred as the lattice is driven around a compression cycle. This energy is dissipated by the damping acting on the beads and the excitation force at the defect. Since changing the drive amplitude can control the area enclosed in the hysteresis loop, the system can also act as a tunable damper (Fig. 6.4d).

This work allows tuning bulk material properties using the excitation of localized defect modes. We anticipate that these results will extend to a variety of materials containing defects. Several questions remain to be answered. Driving multiple defects at different frequencies presents an opportunity to design materials with an arbitrary stress-strain response. Our analytical model shows that by using different nonlinear couplings it is possible to extend the dynamic range of this technique and achieve positive infinite stiffness (see Appendix 1.1). In two- and three-dimensional materials this mechanism could lead to controllable anisotropy.

6.3 Transient Analysis

In this system we are driving a defect mode and utilizing the changes in the resonance that occurs as we approach the bifurcation. Essential to this phenomenon of tunable stiffness is the assumption that system remains at the steady state response. Each time there is an incremental change in the overall displacement of the lattice, there is also a perturbation to the steady state. This means that changes to the incremental stiffness are limited to lower frequencies. So a natural question that arises is, how slow is slow enough?

In the linear model the time that it takes for a system to relax back to the steady state solution is dictated by the dissipation, i.e., the quality factor of the system. The perturbation that results from compressing the system decays exponentially. The life of the transient is determined by the system dissipation. However, as the nonlinear system approaches the bifurcation, the slope on one side of the resonance becomes steeper. At the bifurcation point the slope is infinite, and there are two solutions. From a stability point of view, at exactly this point the system is on top of a saddle and does not prefer one solution over the other. Therefore a perturbation takes an infinite amount of time to proceed to the next solution. This means that the time it takes perturbations of the system to relax to the steady state is between the linear dissipation time constant and infinity (which occurs only at the bifurcation point).

The incremental stiffness is limited up to a certain cutoff frequency. From the above qualitative argument when the stiffness is only slightly modified (i.e., in a small amplitude case where the linear assumption holds) the system should react at the speed of the dissipation (quickly). However, when the incremental stiffness is being modified more significantly the system is closer to the bifurcation and the perturbations take longer to settle.

Floquet analysis in driven-damped systems is an ideal tool to study the reaction speed of the system. In the context of nonlinear ODE's, Floquet analysis describes a systems relaxation back to a periodic, limit cycle solution. The magnitudes of the Floquet multipliers, λ_i , of a system describe how linear perturbations to a periodic orbit either grow or decay after a single period, T .

$$\mathbf{v}(t + T) = \lambda_i e^{i\phi_i} \mathbf{v}(t). \quad (6.2)$$

This equation relates the solution, \mathbf{v} , of the ODE from one period to the next. The phase, ϕ , indicates a frequency content of the associated multiplier. When there is dissipation the magnitudes of the multipliers are less than one, $\lambda_i < 1$, indicating that the transients decay. This means that a perturbation decays to the time periodic solution with decay factor, λ , each period. We can therefore evaluate an effective time constant that depends on how close the system is to the bifurcation,

$$\tau = \frac{T}{\ln(\lambda_{max})}, \quad (6.3)$$

where T is the period of the driving frequency and λ is the magnitude of the largest Floquet multiplier. It is clear here that as the magnitude of the multiplier approaches one, the denominator goes to zero and the time constant approaches infinity.

As the system approaches the bifurcation (i.e., as the drive amplitude is increased) Floquet multipliers collide along the positive real axis, and one begins to increase in magnitude. The magnitude of the multiplier, or equivalently the time constant, limits the speed at which tuned incremental stiffness can be achieved. As the system reaches the bifurcation, where infinite stiffness occurs, the Floquet multiplier has a magnitude of one and the time constant is undefined.

Figure 6.5 shows the time constants (a), amplitude response (b), and stiffness (c) as the lattice is compressed. The time constant reaches a maximum as the system approaches a bifurcation.

This can be seen in the steepening of the amplitude response. This also corresponds to regions of highly modified incremental stiffness. It is important to emphasize that although we are discussing dynamics from the point of view of being slow enough, the system actually reacts quite fast for many practical applications.

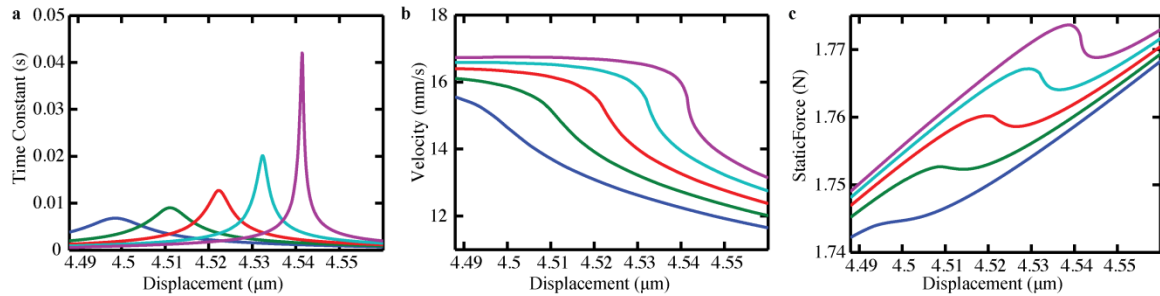


Figure 6.5: Transient Analysis. **a** Time constants that dictate the speed of the relaxation back to steady state. **b** As the system approaches a bifurcation, the amplitude response becomes steeper, and **c** the stiffness is modified more significantly. This is accompanied by longer relaxation time constants, which limits the speed of the system.

In Figure 6.4 we show a band gap at zero frequency. The band gap is not due to a local potential, but instead by tuning the stiffness to zero. This discussion indicates that above a certain frequency the system should not be able to react quickly enough to the perturbations applied by the excitation. We calculate the time constant at the excitation required for the zero frequency band gap, $\tau_0 = 7.807 \text{ ms}$. The time constant that we calculate using Floquet analysis predicts the frequency cutoff remarkably well, $f_\tau = 1/(2\pi\tau) = 20.39$, compared to the frequency cutoff from Figure 6.4, which is calculated from fitting to the first order filter, $f_c = 20.35$. The frequency cutoff here is due to a completely different effect than the linear band gap in a periodic crystal. In a traditional band gap, the wave vector becomes imaginary and is reflected. Here, the stiffness of the system is simply zero.

6.4 Author contribution

The results from this chapter are from “Extraordinary stiffness tunability through thermal expansion of nonlinear defect modes”. Marc Serra-Garcia and Joseph Lydon developed the system concept and contributed equally to the project. Marc Serra-Garcia performed the experimental work and the analytical study. Joseph Lydon developed the numerical analysis. All authors contributed to the analysis of the data and to the writing of the manuscript.